**This paper is published as part of a *Dalton Transactions* themed issue on:**

# Bioinspired Catalysis

Guest Editor Seiji Ogo
Kyushu University, Japan

Published in issue 12, 2010 of *Dalton Transactions*

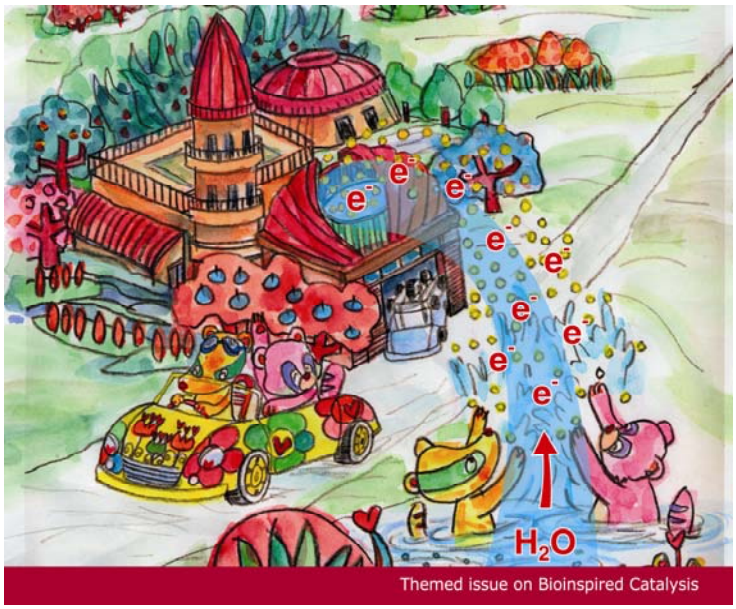


Image reproduced with permission of Seiji Ogo

Articles published in this issue include:

**PERSPECTIVES:**

Mimicking Nitrogenase
Ian Dance
*Dalton Trans.,* 2010, DOI: 10.1039/b922606k

Dual functions of NifEN: insights into the evolution and mechanism of nitrogenase
Yilin Hu, Aaron W. Fay, Chi Chung Lee, Jared A. Wiig and Markus W. Ribbe
*Dalton Trans.,* 2010, DOI: 10.1039/b922555b

Quest for metal/NH bifunctional biomimetic catalysis in a dinuclear platform
Takao Ikariya and Shigeki Kuwata
*Dalton Trans.,* 2010, DOI: 10.1039/b927357c

**COMMUNICATION:**

Chemiluminescence enhancement and energy transfer by the aluminium(III) complex of an amphiphilic/bipolar and cell-penetrating corrole
Atif Mahammed and Zeev Gross
*Dalton Trans*., 2010, DOI: 10.1039/b916590h

Visit the *Dalton Transactions* website for more cutting-edge inorganic and bioinorganic research
www.rsc.org/dalton

# Reduction of oxygen catalyzed by nickel diphosphine complexes with positioned pendant amines†

**Jenny Y. Yang,[a] R. Morris Bullock,[a] William G. Dougherty,[b] W. Scott Kassel,[b] Brendan Twamley,[c] Daniel L. DuBois*[a] and M. Rakowski DuBois*[a]**

***Received 12th October 2009, Accepted 30th November 2009***
***First published as an Advance Article on the web 19th January 2010***
**DOI: 10.1039/b921245k**

Nickel(II) bis(diphosphine) complexes that contain positioned bases in the second coordination sphere have been found to catalyze the reduction of $O_2$ with $H_2$ to selectively form water. The complexes also serve as electrocatalysts for the reduction of $O_2$ with the addition of a weak acid. In contrast, a closely related nickel diphosphine complex without the positioned bases is catalytically inactive for $O_2$ reduction. These results indicate that pendant bases in synthetic catalysts for $O_2$ reduction can play a similar role to proton relays in enzymes, and that such relays should be considered in the design of catalysts for multi-electron and multi-proton reactions.

## Introduction

Hydrogenase enzymes promote the interconversion of molecular hydrogen and protons at high rates and demonstrate that first row transition metals are viable catalysts for this important reaction. Recent structural studies of the FeFe hydrogenases have established that the active site contains two iron centers bridged by a dithiolate ligand and coordinated by terminal carbonyl and cyanide ligands.[1] The structural studies have led to the suggestion that a basic nitrogen or oxygen atom may be incorporated into the backbone of the dithiolate ligand.[1-4] The positioning of the base in the second coordination sphere of the active site is proposed to facilitate the cleavage/formation of the hydrogen–hydrogen bond and the transfer of protons to and from the reactive metal center. In our laboratories this suggestion inspired efforts to determine how bases in the second coordination sphere of simple synthetic diphosphine complexes of nickel, cobalt and iron might influence their interactions with protons and with dihydrogen. Our studies have provided well-documented examples of how positioned amine bases in the second coordination sphere function as effective proton relays and promote hydrogen activation, and have led to the development of very active electrocatalysts for hydrogen formation and oxidation. This work has been reviewed recently.[5] An important corollary of these studies is that proton relays, positioned in the second coordination sphere, should be important in the design of synthetic catalysts for other multi-electron/proton transfer processes, for example in reactions that are important in the development of alternative fuels.

An important challenge facing the widespread application of fuel cells is the cost and efficiency of the material components.[6] A crucial target is improving the oxygen reduction reaction catalyst at the cathodic end of hydrogen- and direct methanol- based fuel cells, as it is the most important factor limiting overall performance and price. Currently, the most commonly used electrode material is Pt, although a number of materials are being explored to reduce[7-9] or eliminate[10-13] the need for this expensive metal. The coupling of oxygen reduction to fuel oxidation is not unique to fuel cell applications; it is also the foundation of biological aerobic energy generation. Efficient and rapid reduction of oxygen is carried out without the use of noble metals in nature by cytochrome *c* oxidase enzymes to power the cellular proton pump during the final stage of respiration. The enzymes display high selectivity for the four-electron reduction to water. The latter is an important feature, as the two-step, two-electron reduction that releases hydrogen peroxide as an intermediate is less efficient. Incomplete reduction to water also results in reactive oxygen species such as $O_2^{\bullet-}$, $H_2O_2$, and $OH^{\bullet}$ which are detrimental in both biological systems and fuel cell applications. The origins of the high selectivity and efficiency of the oxidase enzymes has been extensively investigated by structural[14,15] and spectroscopic studies on the enzymes,[16,17] as well as on synthetic analogues[18,19] of the active site. A key element is the precisely orchestrated series of coupled proton and electron transfer events in the reduction, which is facilitated by acidic or basic amino acid side chains adjacent to the active site and through other hydrogen-bonding interactions in the second coordination sphere,[20-22] a recurring theme in redox active enzymes.

The molecular nickel complexes that serve as electrocatalysts for hydrogen oxidation and production developed previously in our laboratory, $[Ni(P^R_2N^{R'}_2)_2](BF_4)_2$ (**1–3**) contain two cyclic diphosphine ligands with two amine bases positioned within 3.3 Å from the nickel ion.[23,24] We have shown that the incorporation of two positioned relays

[a]*Chemical and Materials Sciences Division, Pacific Northwest National Laboratory, Richland, WA 99352, USA. E-mail: mary.rakowskidubois@pnl.gov*
[b]*Department of Chemistry, Villanova University, Villanova, Pennsylvania 19085, USA*
[c]*Department of Chemistry, University of Idaho, Moscow, Idaho 83844, USA*

† Electronic supplementary information (ESI) available: Experimental data. CCDC reference numbers 751449 and 751450. For ESI and crystallographic data in CIF or other electronic format see DOI: 10.1039/b921245k

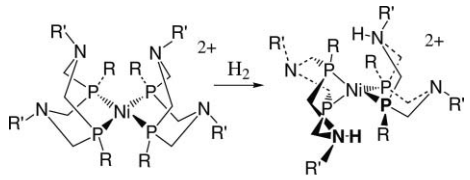

(1)

**1** R = Cy, R' = Bz (benzyl)
**2** R = Ph, R' = Bz
**3** R = Ph, R' = Ph
**4** R = Ph, R' = Me

plays a critical role in promoting both catalytic rates and efficiency in these nickel systems.[25] The heterolytic cleavage of $H_2$ by the nickel complexes has been studied spectroscopically. For example, **1** with R = cyclohexyl and R′ = benzyl, reacts rapidly and completely under an atmosphere of hydrogen to form a $Ni^0$ complex with two protonated bases in close proximity to the metal, as shown in eqn (1).[24] Similarly, the mixed ligand complex $[Ni(P^{Ph}_2N^{Bz}_2)(dppp)](BF_4)_2$ (**5**, where dppp is bis(diphenylphosphinopropane)) reacts with $H_2$ to form a $Ni^0$ complex with both amines of the $P^{Ph}_2N^{Bz}_2$ ligand protonated.[25] These results prompted us to question whether the reduced complexes are capable of delivering protons and electrons to an additional substrate. Although we anticipated that these reduced phosphine complexes would not show long term stability in the presence of $O_2$, the well defined nature of the reduced species in these systems provides an opportunity to explore the importance of positioned proton relays in $O_2$ reduction. In this work, we describe the selective catalytic reduction of $O_2$ to water using this class of nickel complexes and our studies of the role of the pendant bases in the catalytic reactions.

## Results and discussion

### Syntheses

Complexes **1–3**, **5**, and $[Ni(dedpe)_2](BF_4)_2$ (where dedpe is 1-(diethylphosphino)-2-(diphenylphosphino)ethane) were synthesized as previously described in the literature.[23-27] The new cyclic ligand $P^{Ph}_2N^{Me}_2$ was synthesized using a method similar to that used for previously reported $P_2N_2$ type ligands,[23-26,28] but attempts at purification of the crude product mixture were unsuccessful. As a result, the reaction of the crude ligand with the precursor $[Ni(MeCN)_6](BF_4)_2$ to form $[Ni(P^{Ph}_2N^{Me}_2)_2(CH_3CN)](BF_4)_2$ (**4**) also resulted in a product mixture that was difficult to purify. However, addition of hydrogen along with the base tetramethylguanidine to the mixture containing **4** resulted in selective precipitation of the pure Ni(0) complex, $Ni(P^{Ph}_2N^{Me}_2)_2$ (**6**), in low yields. The $^{31}P\{^1H\}$ NMR spectrum of this complex in acetonitrile consists of a single resonance at 1.8 ppm similar to other $Ni^0$ complexes of this type,[25] and the $^1H$ NMR spectrum is also consistent with the formation of the desired complex (see Experimental). A single crystal X-ray diffraction study of **6** was performed, and a drawing of the complex can be seen in Fig. 1. The overall structure is that of a distorted tetrahedron with two chelating $P^{Ph}_2N^{Me}_2$ ligands as expected. Selected bond angles and bond distances for this complex are given in Table 1.

Addition of the acid 4-methoxyanilinium tetrafluoroborate to $Ni(P^{Ph}_2N^{Me}_2)_2$ (**6**) under nitrogen resulted in the slow liberation of hydrogen over two days and provides a route to the clean formation of $[Ni(P^{Ph}_2N^{Me}_2)_2(CH_3CN)](BF_4)_2$ (**4**). The $^{31}P\{^1H\}$ NMR

**Table 1** Selected bond distances (Å) and angles (°) for $Ni(P^{Ph}_2N^{Me}_2)_2$, **6**

| Bond distances | | Bond angles | |
|---|---|---|---|
| Ni(1)–P(1) | 2.1266(4) | P(2)–Ni(1)–P(2)$^i$ | 130.57(3) |
| Ni(1)–P(2) | 2.1262(4) | P(2)–Ni(1)–P(1) | 86.532(14) |
| Ni(1)–N(1) | 3.716 | P(2)$^i$–Ni(1)–P(1) | 120.121(14) |
| Ni(1)–N(2) | 3.378 | | |

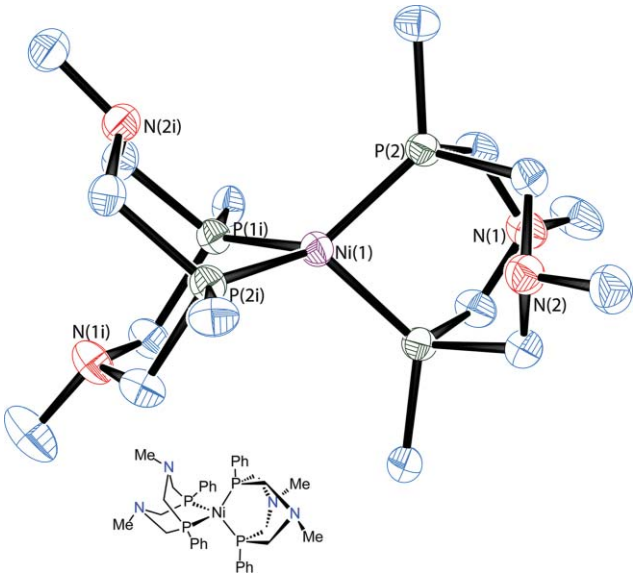


**Fig. 1** Structure of $Ni(P^{Ph}_2N^{Me}_2)_2$ (**6**) showing the atom-numbering scheme. Thermal ellipsoids are shown at the 80% probability level. For clarity, only *ipso* carbons of phenyl rings are shown.

spectrum of this complex at room temperature in acetonitrile is similar to those of other $Ni^{II}$ complexes of this type,[23,26] and consists of a broad resonance at 7.9 ppm. Based on previously studied analogues, the gross geometry is expected to be a trigonal bipyramid. The broad resonance observed is due to the fluxional nature of the five-coordinate complex, which can undergo a Berry pseudorotation to exchange axial and equatorial phosphorus atoms. Cooling the complex below –20° C slows the exchange so the axial and equatorial phosphines can be distinguished. The variable temperature $^{31}P$ NMR spectra are shown in Fig. S1, ESI.† The $^1H$ NMR spectrum is also consistent with the formation of the desired complex (see Experimental). Cyclic voltammograms recorded on **4** (see below) are identical with those of complex **6**, consistent with a simple oxidation of **6** by two electrons to form **4**.

### Stability of the nickel(II) complexes to oxygen and hydrogen peroxide

As discussed in the introduction, we were interested in using the protonated Ni(0) complexes resulting from $H_2$ activation (eqn (1)) as catalysts for $O_2$ reduction. For this application the Ni(II) derivatives must be stable to oxygen (or react with this reagent more slowly than they react with hydrogen). A solution of $[Ni(P^{Cy}_2N^{Bz}_2)_2](BF_4)_2$ (**1**) in acetone was purged with oxygen for 10 min and monitored by $^{31}P\{^1H\}$ NMR spectroscopy to determine its stability under these conditions. About 10% of the original complex decomposed over 6 h, as indicated by the appearance of a new resonance at 36 ppm in the $^{31}P$ NMR spectrum. In contrast,

 

the phenyl substituted phosphine complexes **2–4** and the control complex, $[Ni(dedpe)_2](BF_4)_2$, which lacks pendant bases, are stable in air for weeks without decomposition detectable by $^{31}P\{^1H\}$ NMR. The mixed ligand complex $[Ni(P^{Ph}_2N^{Bz}_2)(dppp)](BF_4)_2$ (**5**) is moderately sensitive to oxygen; over the course of one hour about 20% of the complex decomposes to form $[Ni(P^{Ph}_2N^{Bz}_2)_2](BF_4)_2$ and oxidized diphenylphosphinopropane. Similarly, the previously studied complex $[Ni(PNP)_2](BF_4)_2$ (**7**) (where PNP = bis(diethylphosphinomethyl)methylamine) was considered for study because it reacts readily with hydrogen to form a nickel hydride complex with a protonated pendant amine.[29] However, **7** also decomposes within minutes upon purging with air as determined by $^{31}P\{^1H\}$ NMR spectroscopy. As a result, studies of **5** and **7** were not pursued further.

If the reduction of oxygen to water proceeds *via* a two-step, two-electron process, hydrogen peroxide could be released as an intermediate product. The stability of the nickel(II) complexes **1–4** to hydrogen peroxide was examined by monitoring a solution of each complex in acetonitrile by $^{31}P\{^1H\}$ NMR spectroscopy upon addition of 30% aqueous hydrogen peroxide (10 equivalents). No decomposition was observed for derivatives **2–4** over the course of an hour. An analogous study of **2** was carried out using urea hydrogen peroxide as an anhydrous hydrogen peroxide source, and again, no evidence for decomposition was observed in the $^{31}P\{^1H\}$ NMR spectrum. Complex **1** reacted with aqueous $H_2O_2$ in acetonitrile with 80% decomposition over 1 h.

### Reduction of $O_2$ with hydrogen

On the basis of the studies described above, complexes **1–4** were found to be sufficiently stable to oxygen to merit further study as catalysts for the reduction of $O_2$ by $H_2$. In addition to oxygen stability in the Ni(II) state, potential catalysts for this reaction must also react readily with hydrogen. Previous studies have shown that complex **1** reacts reversibly with one atm $H_2$ to form the Ni(0) complex shown in eqn (1) and, at room temperature, two other isomers in which an amine in each cyclic ligand is protonated.[24] Similar species were observed for complex **2**, but higher $H_2$ pressures were required for their formation.[26] The equilibrium constants determined for these reactions at 22 °C are shown in column 2 of Table 2. In contrast, **3** does not react with $H_2$ under these conditions, consistent with the estimated binding constant for this complex of $2 \times 10^{-6}$ $atm^{-1}$.[23] The new complex $[Ni(P^{Ph}_2N^{Me}_2)_2](BF_4)_2$ (**4**) was synthesized in an effort to prepare an oxygen stable derivative that had a higher $H_2$ binding constant than those for **2** or **3**.

$^{31}P\{^1H\}$ NMR spectroscopy confirms that **4** under 1.0 atm of $H_2$ in acetonitrile at room temperature forms an equilibrium mixture of **4** and isomeric products analogous to those observed previously for **1**[24] (see Experimental for details). Integration of the $^{31}P\{^1H\}$ resonances assigned to these species gives an equilibrium constant for $H_2$ binding to **4** of 6.1 $atm^{-1}$ in acetonitrile at 20 °C. As can be seen from Table 2, this binding constant is smaller than that of **1** but greater than those of **2** and **3**. In summary, **1** and **4** have binding constants sufficiently large to favor hydrogen addition under one atmosphere (see Table 2), and **2** will form low concentrations of the diprotonated Ni(0) isomers under these conditions.

To assess the ability of complexes **1–4** to catalyze the reduction of oxygen by hydrogen and to determine the nature of the product(s), the reactions were monitored by $^2H$ NMR spectroscopy using deuterium gas as the reductant. For example, in a typical set of conditions, a 10 mM acetonitrile solution of $[Ni(P^{Ph}_2N^{Bz}_2)_2](BF_4)_2$ (**2**) was prepared in an NMR tube under $D_2$ (90 μmol) and 90 μmol $O_2$ was added. Deuterobenzene was added as an internal standard. The $D_2O$ resonance at 2.44 ppm grows over the course of an hour at room temperature as shown in Fig. 2. There is no evidence of $D_2O_2$ or other products in the $^2H$ NMR spectra, and separate control experiments indicate $H_2O$ and $H_2O_2$ exhibit separate resonances at 2.2 and 8.7 ppm, respectively, under these conditions. After 1 h, 80 μmol of $D_2O$ is observed, equivalent to 7 turnovers based on the initial amount of **2** as the catalyst. Catalytic activity is not maximized under these conditions, as the turnover frequency is limited by the slow diffusion of the two gaseous reagents and by the limited volume of the NMR tube (as well as by catalyst decomposition, see below). Nevertheless these studies confirm that the reaction proceeds catalytically with the selective formation of water. Similar studies were carried out for complexes **1**, **3**, and **4**. In each case low activity for the conversion of $O_2$ to $H_2O$ was observed, but the turnover number was smaller than that observed for **2**. These values are summarized in Table 2, column 3.

**Table 2** Equilibrium constants for $H_2$ addition to nickel complexes and turnover numbers for water formation

| Complex (RR′) | $K_{eqn\ (1)}$[a] | TON $(D_2O)$[b] |
|---|---|---|
| **1** (CyBz) | $1.9 \times 10^2$ | 1 |
| **2** (PhBz) | $1.3 \times 10^{-2}$ | 7 |
| **3** (PhPh) | $2.0 \times 10^{-6}$ | < 0.2 |
| **4** (PhMe) | 6.1 | 3 |
| $[Ni(dedpe)_2](BF_4)_2$[c] | | 0 |

[a] Equilibrium constants determined from measured or estimated free energy of hydrogen addition under one atmosphere, from ref. 26 for compounds **1–3**. [b] TON determined by equivalents of $D_2O$ generated after the catalyst is mixed with $D_2$ and $O_2$ for one hour, as described in the Experimental section. [c] Reaction was run with 10 equivalents of $Et_3N$ relative to the complex.

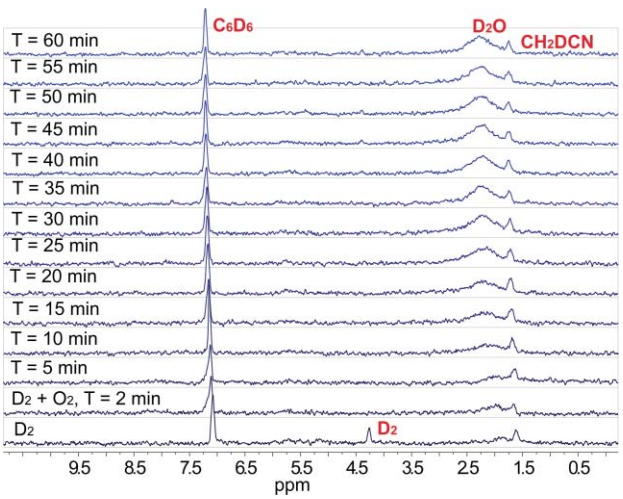


**Fig. 2** $^2H$ NMR spectra of a 10.4 mM solution of **2** in $CH_3CN$ under deuterium (bottom), and after addition of oxygen. $C_6D_6$ was added as an internal reference.

In order to determine whether the positioned bases in the second coordination spheres of these complexes are important for

**Table 3** Selected bond distances (Å) and bond angles (°) for **8**

| Bond distances | | | | Bond angles | |
|---|---|---|---|---|---|
| Ni(1)–O(1) | 2.0507(17) | O(1)–P(1) | 1.5063(18) | O(1)–Ni(1)–O(4) | 90.47 |
| Ni(1)–O(2) | 2.0421(18) | O(2)–P(2) | 1.5139(18) | O(3)–Ni(1)–O(4) | 87.28 |
| Ni(1)–O(3) | 2.0512(17) | O(3)–P(3) | 1.5059(18) | O(1)–Ni(1)–N(24) | 87.25 |
| Ni(1)–O(4) | 2.0504(18) | O(4)–P(4) | 1.5110(18) | O(1)–Ni(1)–N(56) | 90.97 |
| N(24)–Ni(1) | 2.172(2) | | | O(2)–Ni(1)–N(24) | 89.47 |
| N(56)–Ni(1) | 2.180(2) | | | O(2)–Ni(1)–N(56) | 91.31 |
| | | | | O(3)–Ni(1)–N(24) | 94.22 |
| | | | | O(3)–Ni(1)–N(56) | 87.52 |

the catalytic activity, $[Ni(dedpe)_2](BF_4)_2$, which lacks a pendant base, was studied under the same conditions (90 μmol $O_2$ and 90 μmol $H_2$) using a 10 fold excess of triethylamine as a base. Under these conditions, the heterolytic cleavage of $H_2$ to form $[HNi(dedpe)_2](BF_4)$ and $[HNEt_3](BF_4)$ is thermodynamically favorable by approximately 8 kcal $mol^{-1}$, but requires 24 h to achieve 70% conversion.[27] In the presence of $H_2$, $O_2$, and $Et_3N$, conversion of $[Ni(dedpe)_2](BF_4)_2$ to $[HNi(dedpe)_2](BF_4)$ (70%) and $Ni(dedpe)_2$ (30%) was observed by $^{31}P\{^1H\}$ NMR spectroscopy after 24 h. However in this case no $D_2O$ or $D_2O_2$ was detected by NMR spectroscopy after 24 h.

Although $D_2O_2$ was never observed in any of the NMR studies, this does not preclude it as an intermediate. Hydrogen peroxide generated by a two electron reduction could either be reduced by the catalyst using another equivalent of hydrogen as shown in Scheme 1 (*via* path b), or alternatively, the nickel complex could serve as a catalyst for the disproportionation of $H_2O_2$ into water and oxygen (Scheme 1, path c, *i.e.* catalase activity). Both of these possibilities were tested. Urea hydrogen peroxide (14 equivalents), which is only sparingly soluble in acetonitrile, was added to a solution of **2** in $CD_3CN$. Upon purging the solution with hydrogen, the urea hydrogen peroxide dissolved in less than a minute, and the $^1H$ NMR spectrum confirmed the reduction of hydrogen peroxide to water (reaction b). All of the urea hydrogen peroxide, most of which was initially undissolved, was consumed upon addition of hydrogen. The catalyst was also tested for activity towards the disproportionation of hydrogen peroxide (reaction c). $H_2O_2$ (30 wt.% in water, 2100 equivalents) was added to an acetonitrile solution of **2** in a vial fitted to an inverted burette to measure gas evolution. No oxygen was generated from the reaction over the course of one hour. Based on these results, pathways c and d can be excluded, but oxygen reduction could be proceeding *via* the four-electron reduction with no intermediates (a), or *via* a sequential two-electron pathway involving hydrogen peroxide as an intermediate that is reduced by a second nickel complex.

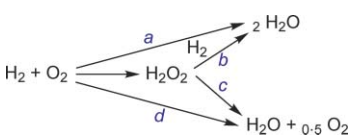


**Scheme 1** Possible pathways for water formation.

## Catalyst decomposition

Although $[Ni(P^{Ph}{}_2N^{Bz}{}_2)_2](BF_4)_2$ (**2**) was found to be stable to oxygen for extended periods and to $H_2O_2$ for over an hour, the $^{31}P\{^1H\}$ NMR spectra taken after this complex was exposed to a mixture of $D_2$ and $O_2$ for one hour indicates most of the starting compound has decomposed over the course of the experiment. These observations indicate that the observed decomposition is the result of the reaction of $O_2$ or $H_2O_2$, produced during the course of the catalytic reaction, with an intermediate species and not with the initial Ni(II) complex. The decomposition product has been independently prepared by exposing an acetonitrile solution of the parent compound **2** to a mixture of hydrogen and oxygen for one day. The oxidized product can be isolated by recrystallization and displays a broad resonance at 66 ppm in the $^{31}P\{^1H\}$ NMR spectrum. The structure was determined by single crystal X-ray analysis to be $[Ni(O_2P^{Ph}{}_2N^{Bz}{}_2)_2](BF_4)_2{\cdot}CH_3CN$ (**8**), and the crystals were shown to consist of a discrete octahedral dication, with two $BF_4^-$ anions, and an uncoordinated acetonitrile molecule. Selected bond distances and angles are given in Table 3, and a drawing of the dication showing the atom numbering scheme for selected atoms is shown in Fig. 3.

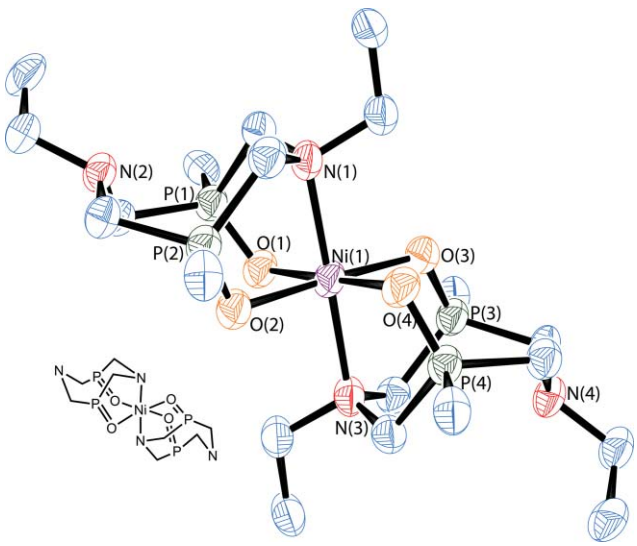


**Fig. 3** Structure of $[Ni(O_2P^{Ph}{}_2N^{Bz}{}_2)_2](BF_4)_2{\cdot}CH_3CN$ (**8**) showing the atom-numbering scheme. Thermal ellipsoids are shown at the 80% probability level. For clarity, only *ipso* carbons of phenyl rings are shown, and the counterions and acetonitrile molecule are not included in this drawing.

In this complex, all four phosphines have been oxidized to phosphine oxides while the remainder of each cyclic ligand remains intact. The oxidized ligands bind to the Ni(II) ion through the oxygens to form eight-membered chelate rings, and an amine from

 

**Table 4** Reduction potentials in acetonitrile for the catalysts examined for oxygen reduction activity

| Complex | $E_{1/2}$ Ni(II/I) | $E_{1/2}$ Ni(I/0) |
|---|---|---|
| $Ni(P^{Cy}_2N^{Bz}_2)_2(BF_4)_2$ (**1**) | –0.80 | –1.28 |
| $Ni(P^{Ph}_2N^{Bz}_2)_2(BF_4)_2$ (**2**) | –0.94 | –1.19 |
| $Ni(P^{Ph}_2N^{Ph}_2)_2(BF_4)_2$ (**3**) | –0.84 | –1.02 |
| $Ni(P^{Ph}_2N^{Me}_2)_2(BF_4)_2$ (**4**) | –0.98 | –1.14 |
| $Ni(dedpe)_2(BF_4)_2$ | –0.99 | –1.08 |

All potentials are in volts *versus* the ferrocenium/ferrocene couple in acetonitrile.

each ligand is coordinated to the *trans* sites of the octahedron. This product is stable to oxygen and does not react with hydrogen.

## Electrochemical studies

Each of the $[Ni(P^R_2N^{R'}_2)_2](BF_4)_2$ derivatives is well behaved electrochemically and shows two reversible one-electron reductions corresponding to the Ni(II/I) and Ni(I/0) couples. The half-wave potentials for **1–3** have been reported previously[23,26] and are presented in Table 4 along with data for the new complex **4** and for $[Ni(dedpe)_2](BF_4)_2$. The latter complex, with no pendant amines, was chosen for comparisons in this work because its reduction potentials are very similar to those of **1–4**.

Because $[Ni(P^{Ph}_2N^{Bz}_2)_2](BF_4)_2$ (**2**) provided the highest turnover number in the reactions of hydrogen and oxygen to form water, a series of experiments were performed to see if this complex is also an electrocatalyst for $O_2$ reduction in the presence of acid. Fig. 4 shows a series of cyclic voltammograms under various conditions that were designed to probe this question. The black trace in Fig. 4 is a cyclic voltammogram of **2** in acetonitrile under one atmosphere of nitrogen. In this case, the two reversible one-electron reductions are observed, as described above. The wave at 0.0 V is the ferrocenium/ferrocene reference couple added as an internal standard. The solid red trace displays a cyclic voltammogram of the same solution upon purging with oxygen.

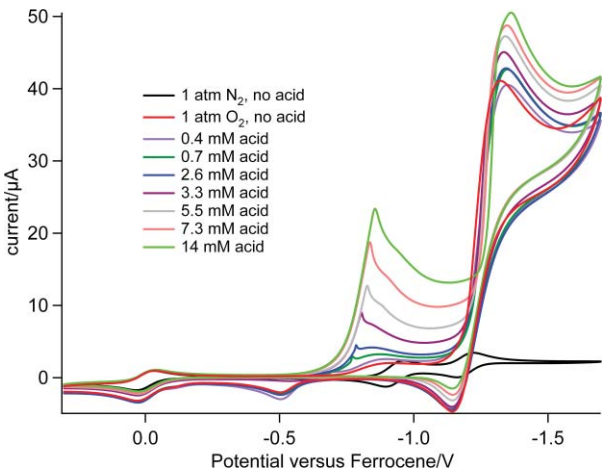


**Fig. 4** Successive cyclic voltammograms of a 1.7 mM solution of $[Ni(P^{Ph}_2N^{Bz}_2)_2](BF_4)_2$ (**2**) at increasing concentrations of 4-bromoanilinium tetrafluoroborate, as indicated in the legend. Conditions: scan rate = 50 mV $s^{-1}$, acetonitrile solvent, 0.2 M $Et_4NBF_4$ as supporting electrolyte, glassy carbon working electrode. Potentials are referenced to the ferrocene/ferrocenium couple (wave shown at 0.0 V).

The large wave observed at –1.27 V at the glassy carbon electrode is assigned to the uncatalyzed one-electron reduction of oxygen to superoxide, and it can be seen that this wave also occurs at potentials similar to those of the Ni(I/0) couple. In the absence of **2**, the $O_2/O_2^-$ couple is more reversible, suggesting possible reactions of the $O_2^-$ ion with Ni(I) or Ni(0). This aspect was not pursued further. It can also be seen from the solid red trace that the wave corresponding to the Ni(II/I) couple shifts from –0.94 V to a more positive potential ($E_p$ = –0.78 V) and becomes irreversible in the presence of $O_2$. This indicates that the reduction of Ni(II) to Ni(I) is followed by a fast irreversible reaction of the Ni(I) cation with $O_2$.

The remaining traces in Fig. 4 show cyclic voltammograms of **2** recorded in acetonitrile solutions saturated with $O_2$ at different concentrations of the acid 4-bromoanilnium tetrafluoroborate. It can be seen that a catalytic current is observed with increasing concentrations of the acid. A sharp current spike is observed on the rising portion of the catalytic wave that is present only when both $O_2$ and $H^+$ are present, and this feature is attributed to a surface confined species. At acid concentrations significantly greater than those shown in Fig. 4, the $O_2/O_2^-$ couple shifts to more positive potentials and begins to overlap the catalytic wave. Because of complexities introduced by the presence of the current spike, the low concentration of oxygen in solution, and interference from the $O_2/O_2^-$ couple at high acid concentrations, a quantitative analysis of the catalytic $O_2$ reduction reaction was not attempted. However, as can be seen from a comparison of the magnitude of the currents at approximately –0.8 V in the absence of acid ($i_p$) and in the presence of 14 mmol acid ($i_c$), this nickel complex is a very active catalyst for the reduction of $O_2$ under acidic conditions with an $i_c/i_p$ ratio of roughly 20 : 1. The CV data also show that the catalytic rate is dependent on the concentration of acid. As discussed in the supporting information, the catalytic current under pure oxygen is about three times larger than the current under air, indicating an oxygen dependence as well.† Finally, the catalytic current is initially dependent on catalyst concentration, but quickly becomes independent of concentration above approximately 1.0 mM (see Fig. S2, ESI†). This is consistent with the formation of a catalytic intermediate that is confined to the surface of the electrode and whose concentration is limited by the coverage of the electrode surface and not the bulk concentration. Taken together, these data indicate that the reduction of the Ni(II) species to form a Ni(I) complex is followed by reaction with $O_2$ and protons to form a catalytic species that binds to the electrode surface. In studies with other types of supporting ligands, reactions of Ni(I) complexes with $O_2$ have been investigated, and a variety of bonding modes for the Ni–$O_2$ products have been characterized.[30] Unfortunately, the adsorption of the catalytic intermediate onto the electrode surface made studies of this intermediate using conventional spectroscopic techniques for homogeneous species of little use. Attempts to detect $H_2O_2$ as a transient intermediate product using rotating ring/disk experiments were ambiguous for homogeneous solutions of the catalysts, and attempts to observe redox chemistry of **2** adsorbed directly on a glassy carbon disk were unsuccessful.

To confirm catalytic reduction of oxygen, a controlled potential electrolysis was performed at –0.90 V on a solution containing **2** and excess *d*-bromoanilinium triflate in a sealed flask. After passing 200 equivalents of charge per mole of **2**, a sample of the solution was removed and the water concentration was

estimated using $^{1}H$ and $^{2}H$ NMR spectroscopy as described in the Experimental section. A current efficiency of 63% was calculated for water production assuming two electrons are required for each water molecule. This corresponds to a turnover number of 63 for $H_2O$ production. Control experiments under various conditions are presented in the supporting information. For example, **2** is a relatively slow electrocatalyst for proton reduction, and the catalytic wave observed for **2** under an $O_2$ atmosphere is much larger than that observed for hydrogen formation by this complex in the absence of $O_2$ (shown in Fig. S3†). Nevertheless, the less then 100% current efficiency for $H_2O$ production observed in the above electrolysis experiment is likely attributable to a competing reduction of protons to produce hydrogen. In a second control experiment (data shown in Fig. S4†) it was established that **2** does not catalyze the reduction of acidic solutions of $H_2O_2$ at comparable rates to the reduction of $O_2$ observed in Fig. 4.

### Comparison of different complexes for electrocatalytic $O_2$ reduction

Fig. 5 displays the current observed for complexes **2**, **3**, and **4**, as well as $[Ni(dedpe)_2](BF_4)_2$ in acetonitrile solutions of 4-bromoanilinium tetrafluoroborate (about 8.5 equivalents of acid) under one atm of $O_2$. All of the complexes display an increase in current in the presence of acid and oxygen. $[Ni(dedpe)_2](BF_4)_2$ (black) and $[Ni(P^{Ph}_2N^{Ph}_2)_2](BF_4)_2$ (**3**) (green) show very small current increases that are not consistent with rapid catalytic $O_2$ reduction. In the case of **3**, the acid, 4-bromoanilinium tetrafluoroborate, is not strong enough to protonate the pendant base,[31] and so the electrochemical response of this complex is similar to the case where no pendant base is present. A more significant catalytic current is observed for $[Ni(P^{Ph}_2N^{Me}_2)_2](BF_4)_2$ (**4**), and the largest current response is observed for $[Ni(P^{Ph}_2N^{Bz}_2)_2](BF_4)_2$ (**2**). Both of these complexes contain positioned basic amines that are capable of functioning as proton relays.

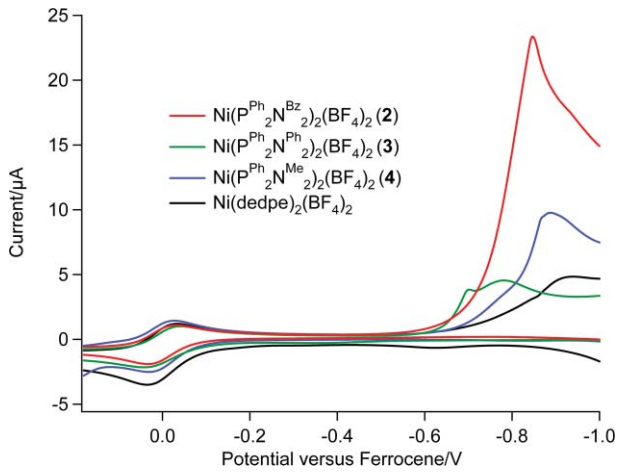


**Fig. 5** Cyclic voltammograms of 1.7 mM solutions of $[Ni(P^{Ph}_2N^{Bz}_2)_2](BF_4)_2$ (**2**) (red), $[Ni(P^{Ph}_2N^{Ph}_2)_2](BF_4)_2$ (**3**) (green), $[Ni(P^{Ph}_2N^{Me}_2)_2](BF_4)_2$ (**4**) (blue), and $[Ni(dedpe)_2](BF_4)_2$ (black) and 14.5 mM of 4-bromoanilinium tetrafluoroborate under 1 atmosphere of oxygen. Conditions: scan rate = 50 mV $s^{-1}$, acetonitrile solvent, 0.2 M $Et_4NBF_4$ as supporting electrolyte, glassy carbon working electrode. Potentials are referenced to the ferrocene/ferrocenium couple (wave shown at 0.0 V).

## Discussion

### Catalyzed reactions of $H_2$ and $O_2$

Examples of molecular hydrogenation catalysts for the reduction of $O_2$ to form $H_2O$ have been reported recently that make use of an amine base in the primary coordination sphere of the metal. For example, the iridium(III) complex with the protonated diimido ligand, $[Cp^*IrNH_2C(Ph)C(Ph)NTs]^+$, is found to react with $H_2$ to form an Ir-hydride species, and the reduction of $O_2$ involves the transfer of the hydride ligand and a proton from the amino group of the bidentate ligand.[32] Because the reduction product is water, two molecules of catalyst are involved in the overall process. The catalyst is found to degrade by the formation of fulvene derivatives. More recently the role of the dinuclear rhodium imido complex, $[Cp^*Rh(\mu\text{-}NTs)]_2$, in the reduction of $O_2$ to $H_2O$ has also been reported.[33] In this case the catalyst adds $H_2$ to ultimately form a Rh(II) product with μ-amido ligands, and then transfers two protons from the bridging ligands and an electron from each metal center to $O_2$ to form water and regenerate the original Rh(III) dimer. Again two catalyst molecules are required for each turnover to form water. While the rates and turnover numbers for these catalysts are low, the reports illustrate that the incorporation of internal bases is an important aspect of catalyst design.

In the work reported here, nickel complexes that contain positioned amines in the second coordination sphere of the complex have been investigated as $O_2$ reduction catalysts. In previous work the pendant amines in these types of structures have been shown to function as very effective proton relays between the metal center and the solution. In addition these positioned bases have been found to stabilize substrate ($H_2$ and CO) binding interactions with the metal center[24,34] and to participate in proton-coupled electron transfer reactions.[5]

This study demonstrates that nickel diphosphine complexes with two positioned bases in the second coordination sphere can serve as catalysts for the reaction of $H_2$ with $O_2$ to form water, while closely related diphosphine complexes with no pendant amines or with amines of low basicity show no catalytic activity. These results confirm that proton relays can play an essential role in the catalytic reduction of $O_2$. The complexes that function as catalysts have the following characteristics. They are stable to oxygen in the Ni(II) oxidation state, and they react rapidly with $H_2$ at room temperature to form Ni(0) products in which the pendant amine bases of the cyclic ligands have been protonated (see eqn (1)). The most active catalyst in this series is $[Ni(P^{Ph}_2N^{Bz}_2)_2](BF_4)_2$ (**2**). This derivative has a much smaller equilibrium constant for $H_2$ addition than $[Ni(P^{Cy}_2N^{Bz}_2)_2](BF_4)_2$ (**1**) and $[Ni(P^{Ph}_2N^{Me}_2)_2](BF_4)_2$ (**4**). Complex **2** is significantly more stable to oxygen in its Ni(II) state than **1**, and the low concentration of Ni(0) products formed upon addition of hydrogen may also limit the oxidative decomposition of the catalyst relative to **1** and **4**. Nevertheless, catalyst decomposition during the reaction of **2** with the $H_2/O_2$ mixture is significant, and it results from the oxidation of a reduced nickel intermediate to form a Ni(II)complex containing the phosphine oxide form of the cyclic ligands. The catalyst instability clearly contributes to the low turnover numbers for this reaction and points to the need for the design of catalyst systems that are more resistant to oxidation.

No hydrogen peroxide is detected during the course of the catalytic reactions. It is possible that two molecules of catalyst react

 

with the $O_2$ substrate to form the 4-electron reduction product, $H_2O$, without the intermediacy of $H_2O_2$. However independent experiments have shown that **2** catalyzes the rapid reduction of $H_2O_2$ by hydrogen under conditions similar to those used in the formation of $H_2O$, and the transient formation of the two-electron reduction product during the catalytic reaction cannot be ruled out. However we have confirmed that the water formed in this reaction is not the result of the catalytic disproportionation of hydrogen peroxide.

### Electrocatalysts for $O_2$ reduction

Significant research effort has been devoted to the development of electrocatalysts for $O_2$ reduction, and a focus on the four-electron reduction to water is of particular interest because of the utility of this reaction in fuel cells. In many cases the catalyst design has involved the use of complexes containing two positioned metal centers in order to mimic the active site of cytochrome *c* oxidase and achieve the required donation of four electrons.[35-38] Another factor that is proposed to contribute to the activity of cytochrome *c* oxidase is the presence of proton relays, but it seems that few synthetic electrocatalysts have been designed to model this aspect of the reduction process.[39] In closely related work, Nocera and coworkers have described a series of complexes containing positioned pendant acids and have demonstrated the importance of the proton relays in catalase and epoxidation catalysis.[40]

The cyclic voltammograms of the nickel diphosphine complexes studied here, recorded under an atmosphere of $O_2$, show an increase in current at the potential of the Ni(II/I) couple with the addition of a weak acid. The best electrocatalyst in the series of complexes studied is $[Ni(P^{Ph}_2N^{Bz}_2)_2](BF_4)_2$ (**2**), which shows a significant current enhancement in the presence of an approximate 10-fold excess of bromoanilinium tetrafluoroborate. This complex also functioned as the best catalyst for the reaction with $H_2$ and $O_2$. Our electrochemical studies confirm that the catalytic reaction rate shows a dependence on acid and $O_2$ concentrations and indicates that the catalytically active species is adsorbed on the electrode surface. It is interesting that **2** does not catalyze the electrochemical reduction of $H_2O_2$ at rates comparable to $O_2$ reduction under similar conditions. Unfortunately there are several factors that make this system unsuitable for more detailed mechanistic studies, including the adsorption of the catalyst, and the fact that higher acid concentrations cannot be studied because of interference by the peak corresponding to the uncatalyzed reduction of $O_2$.

A smaller catalytic wave for $O_2$ reduction is also observed for $[Ni(P^{Ph}_2N^{Me}_2)_2](BF_4)_2$ (**4**). Both **2** and **4** show good stability in the Ni(II) state under an atmosphere of $O_2$. Although the other two complexes shown in Fig. 5 are also stable under $O_2$, no significant increase in current is observed for $[Ni(dedpe)_2](BF_4)_2$, which contains no pendant bases, or for $[Ni(P^{Ph}_2N^{Ph}_2)_2](BF_4)_2$ (**3**) in which the pendant amines are too weakly basic to be protonated by the acid used in these experiments. The $O_2$ reduction waves observed for **2** and **4** occur at a very negative potential compared to the $O_2/H_2O$ couple, and different types of structures will be needed for the development of more useful catalysts. However the results reported here provide strong evidence that the incorporation of proton relays should be an important feature in further catalyst design.

## Conclusions

Within the series of nickel diphosphine complexes studied here, a catalyst for both the reaction of $H_2$ with $O_2$ to selectively form water and for the electrochemical reduction of $O_2$ with the addition of a weak acid has been identified. Our studies have established that important factors in the catalytic activity include the presence of one or more bases in the second coordination sphere of the complex that are positioned near the metal ion. Furthermore, the proton-accepting and -donating ability of the base must be well matched with the acid and substrate in the catalytic reaction in order to maximize the proton relay function of the base. The design of new, more efficient molecular catalysts for these reactions will include these important proton relay features as well as the use of more oxidatively robust ligands that can be used to tune the redox potentials of the metal center.

## Experimental

### General experimental procedures

$^1H$, $^2H$, and $^{31}P$ NMR spectra were recorded on a Varian Inova spectrometer (500 MHz for $^1H$) at 20 °C unless otherwise noted. All $^1H$ chemical shifts have been internally calibrated to the monoprotio impurity of the deuterated solvent. The $^2H$ NMR spectra were internally calibrated to the monodeutero impurity in the undeuterated solvent used. In the $^2H$ NMR spectra, the D1 was set at 10 s to ensure accurate signal integration based on the pre-determined relaxation time (T1) for $C_6D_6$ and $D_2O$. The $^{31}P$ NMR spectra were proton decoupled and referenced to external phosphoric acid.

All electrochemical experiments were carried out under an atmosphere of nitrogen, air, or oxygen as indicated, in 0.2 M $Et_4NBF_4$ acetonitrile solutions or 0.2 M $Bu_4NBF_4$ benzonitrile solutions. Cyclic voltammetry experiments were performed with a CH Instruments model 660C potentiostat. Ferrocene was used as an internal standard, and all potentials are referenced to the ferrocenium/ferrocene couple.

### Synthesis and materials

All reactions and manipulations were performed under an atmosphere of $N_2$ using standard Schlenk techniques or a glovebox unless otherwise indicated. Solvents were dried using an activated alumina column. Complexes **1–3**,[23,26] **5**,[25] $[Ni(PNP)_2](BF_4)_2$,[29] and $[Ni(dedpe)_2](BF_4)_2$[27] were prepared as reported previously. Urea hydrogen peroxide (97%) was purchased from Aldrich Chemical Co. Ultra high purity grade hydrogen was used (99.999%). The oxygen used was industrial grade.

### $[Ni(P^{Ph}_2N^{Me}_2)_2]$ (6)

Phenylphosphine (2.7 g, 0.024 mol) and 100 mL of degassed ethanol were added to a 250 mL Schlenk flask. *Para*-formaldehyde (1.55 g, 0.051 mol) was added and the reaction was heated to 70 °C for 12 h. After cooling to room temperature, methylamine (3.35 mL of a 30% w/w solution in ethanol) was added and the reaction was again heated to 70 °C for 6 h. After cooling, the solvent was removed under vacuum to give the crude ligand as an oil. The oil (1.043 g) was dissolved in 15 mL of acetonitrile

with 1.086 g of $[Ni(MeCN)_6](BF_4)_2$[41] (2.17 mmol) and stirred at room temperature for 2 days. The solution was purged with hydrogen, and 0.51 mL of tetramethylguanidine (4.34 mmol) was added. Over the course of two days, orange crystalline product precipitated from the reaction solution. The crystals were isolated by filtration, followed by washing with 2 × 2 mL of acetonitrile to give the pure product (0.200 g, 13%). The same method was used to grow single crystals suitable for X-ray diffraction. $\delta_H(CD_3CN)$ 7.92 (8 H, t, $C_6H_5$), 7.16–7.09 (*ca.* 12 H, m, $C_6H_5$), 3.15 (8 H, d, $CH_2$), 2.76 (8 H, m, $CH_2$), 2.35 (12 H, s, $CH_3$). $\delta_P(CD_3CN$, external $H_3PO_4$) 1.8.

### $[Ni(P^{Ph}{}_2N^{Me}{}_2)_2](BF_4)_2$ (4)

$Ni(P^{Ph}{}_2N^{Me}{}_2)_2$ (100 mg, 0.128 mmol) and 4-methoxyanilinium tetrafluoroborate (83 mg, 0.39 mmol) were added to 2 mL of benzene and the reaction was stirred for two days. The reaction was then filtered to isolate a red solid, which was washed with 5 mL of benzene and 5 mL of diethyl ether and dried under vacuum to give the product (65 mg, 58%). $\delta_H(CD_3CN)$ 7.33–6.79 (20 H, m, $C_6H_5$), 3.73 (8 H, s, $CH_2$), 3.35 (8 H, d, $CH_2$), 2.66 (12 H, s, $CH_3$). $\delta_P(CD_3CN$, external $H_3PO_4$) 7.9 (s, br).

### $[Ni(O_2P^{Ph}{}_2N^{Bz}{}_2)_2](BF_4)_2 \cdot CH_3CN$ (8)

$[Ni(P^{Ph}{}_2N^{Bz}{}_2)_2](BF_4)_2$ (**2**) (125 mg, 0.13 mmol) was dissolved in 4 mL of acetonitrile in a 250 mL Schlenk flask. After the flask was purged with hydrogen for 10 min, 40 mL of air was injected and the solution was stirred at room temperature for 24 h. The solvent was removed under vacuum, and the residue was washed with 4 mL of dichloromethane to leave a light green solid. This was recrystallized by diffusion of diethyl ether into an acetonitrile solution of the solid to give the product (90 mg, 54%). The same method was used to grow single crystals suitable for X-ray diffraction. $\delta_P(CD_3CN$, external $H_3PO_4$) 66.4 (br).

### $H_2$ addition to $[Ni(P^{Ph}{}_2N^{Me}{}_2)_2](BF_4)_2$ (4)

A solution of **4** in acetonitrile in an NMR tube was purged with $H_2$ for 10 min and the $^{31}P$ NMR spectra were recorded at −43 °C. $\delta_P(CH_3CN$, external $H_3PO_4)$ $[Ni(P^{Ph}{}_2N^{Me}{}_2)_2](BF_4)_2$ (**4**) (30.2, −12.4), isomer *a* (12.4), isomer *b* ($ABX_2$ spin system with chemical shifts of 15.1 (2P), −4.1, −10), isomer *c* (−8.42). These isomers are similar to those described for $[Ni(P^{Cy}{}_2N^{Bz}{}_2)_2](BF_4)_2$ upon addition of $H_2$.[24] At 20 °C the following spectral data were obtained. $\delta_P(CH_3CN$, external $H_3PO_4)$ $[Ni(P^{Ph}{}_2N^{Me}{}_2)_2](BF_4)_2$ (**4**) 7.9 (br), $H_2$ addition products, 15.2, 14.3, −7.4, −8.6. The ratio of the starting complex to the $H_2$ addition products at 20 °C was determined by integration using the deconvolution program on Varian NMR software. The equilibrium constant for hydrogen addition is 6.1 $atm^{-1}$, which corresponds to a free energy ($\Delta G^\circ_{H_2}$) of −1.1 kcal $mol^{-1}$ for the reaction of gaseous $H_2$ with complex **4** in an acetonitrile solution.

### Stability of complexes 1–4 in the presence of oxygen and hydrogen peroxide

Acetonitrile solutions of complexes **1–4** (approximately 10 mM) and $[Ni(dedpe)_2](BF_4)_2$ were exposed to air and monitored by $^{31}P\{^1H\}$ NMR for 24 h to determine the extent (if any) of decomposition over that period. To test the stability of these complexes to peroxide, 10 μL of 30% w/w $H_2O_2$ was added to 1.0 mL of 10 mM acetonitrile solutions of complexes **1–4** and the reactions were monitored for decomposition by $^{31}P\{^1H\}$ NMR over one hour. The spectra of complex **1** displayed 70% decomposition over an hour, while **2–4** displayed no observable decomposition. The stability of complex **2** to $H_2O_2$ was also studied by adding 5 mg (0.11 mmol) of urea hydrogen peroxide (UHP) to a 1.0 mL solution of **2** (9.1 mM). No decomposition was observed by $^{31}P\{^1H\}$ NMR over the course of one hour.

### Catalytic reduction of $O_2$ with $D_2$

In a representative experiment $Ni(P^{Ph}{}_2N^{Bz}{}_2)_2(BF_4)_2$, **2** (10 mg, 10.4 μmol), was dissolved in 1.0 mL of $CH_3CN$ in an NMR tube, and 1.0 μL of $C_6D_6$ was added as an internal standard. The solution was purged with $D_2$ for 5 min, and a $^2H$ spectrum was taken to determine the background level of $CH_2DCN$ and $D_2O$ in the sample. Oxygen (2.0 mL, 90 μmol) was then added to the NMR tube and the sample was vigorously shaken. $^2H$ spectra were taken at 5 min intervals over 1 h to monitor product formation. Similar experiments were carried out for complexes **1**, **3**, and **4**. The control $[Ni(dedpe)_2](BF_4)_2$ was tested under the same conditions, except 7.6 μL of $Et_3N$ (104 μmol) was added to the solution to serve as an external base to promote $H_2$ addition to the metal complex. The results of these experiments are summarized in column 3 of Table 2.

### Electrocatalytic reduction of oxygen

In a representative experiment, a 2.5 mL aliquot of a 1.67 mM solution of **2** was prepared in a 0.2 M solution of $Et_4NBF_4$ in acetonitrile. The cell was purged with oxygen gas. The solution was then titrated with a 0.92 M acetonitrile solution of 4-bromoanilinium tetrafluoroborate, and cyclic voltammograms were recorded as shown in Fig. 5. Similar experiments were performed for complexes **1**, **3**, **4**, and $[Ni(dedpe)_2](BF_4)_2$. To determine if there is a dependence of the catalytic rate on oxygen concentration, this experiment was repeated for complex **2** in the presence of air instead of oxygen. The peak current in the presence of $O_2$ is 3 times that in the presence of air. Dependence of the catalytic current on complex concentration was also studied by performing the above experiments under oxygen using different concentrations of **2**. It was observed that after an initial increase in the catalytic current with concentration that the current became independent of catalyst concentration above approximately 1.0 mM. The results are shown in Fig. S2.†

### Test for hydrogen peroxide disproportionation catalysis

These reactions were performed at room temperature in polypropylene septa-sealed 20 mL vials equipped with a magnetic stirbar. A cannula needle linked to an inverted graduated burette filled with water was inserted. Complex **2** (0.095 μmol) was dissolved in 1.0 mL of acetonitrile, and 790 μL of 30% aqueous hydrogen peroxide solution was added. No gas evolution was observed over the course of 1 h.

 

### Controlled-potential coulometry

A five-necked flask with two stopcocks having a total volume of 250 mL was used for bulk electrolysis experiments. One neck was a 24/40 joint that accepted a stainless steel 24/40 fitting with an insulated copper wire running through it. To this was attached a cylinder of reticulated vitreous carbon as a working electrode (1 cm diameter by 2.5 cm length). The other two necks of the flask were 14/20 joints. Both were fitted with glass compartments with Vycor frits on the bottom. One was used as the reference electrode; it was filled with a 0.2 M $Et_4NBF_4$ acetonitrile solution and a silver wire was inserted. The other was used as the counter electrode, and it contained 0.2 M $Et_4NBF_4$ in acetonitrile and a nickel-chromium wire. To the cell was added 15 mL of a 0.2 M $Et_4NBF_4$ in acetonitrile. Bromoanilinium-$d_1$ triflate (1.6 g, 0.33M) and $[Ni(P^{Ph}{}_2N^{Bz}{}_2)](BF_4)_2$ (19.2 mg, 1.07 mM) were added to the solution. Controlled-potential coulometry was performed at –0.90 V *versus* a ferrocene/ferrocenium reference. The solution was purged with oxygen throughout the experiment. After 319.9 C of charge was applied, a sample of the solution was removed and analyzed by $^1H$ and $^2H$ NMR. The concentration of water was determined as follows. The water and amine protons display one broad resonance due to rapid proton exchange. The ratio of acid and conjugate base was determined using the chemical shift of the aromatic resonances in the $^1H$ NMR spectra. The observed shift is a weighted average of the shifts of the protonated base and the free base. A solution with the same acid/base ratio as observed in the electrolysis cell was titrated with water to determine the effect of water concentration on the shift of the protonated amine resonance (see Fig. S4†). A water concentration of 0.07 M was determined using this relationship corresponding to 63 turnovers and a current efficiency of 63%. Because a purge of $O_2$ was used to maintain a high local concentration of $O_2$ at the electrode surface, hydrogen produced in a competing reaction at the electrode is also swept away before it can reduce $O_2$. This results in a current efficiency of less than 100% for $O_2$ reduction.

### X-Ray diffraction studies

A suitable crystal of **8** was selected, attached to a glass fiber and data were collected at 90(2) K using a Bruker/Siemens SMART APEX instrument (Mo Kα radiation, $\lambda = 0.71073$ Å) equipped with a Cryocool NeverIce low temperature device. Data were measured using omega scans 0.3° per frame for 10 s, and a full sphere of data was collected. A total of 2400 frames were collected with a final resolution of 0.83 Å. Cell parameters were retrieved using SMART[42] software and refined using SAINTPlus[43] on all observed reflections. Data reduction and correction for Lp and decay were performed using the SAINTPlus software. Absorption corrections were applied using SADABS.[44]

The structure was solved by direct methods and refined by least squares method on $F^2$ using the SHELXTL program package.[45] The structure was solved in the space group $P2_1/n$ (# 14) by analysis of systematic absences. The diffraction contribution from a disordered $Et_2O$ solvent molecule was removed from the data using the SQUEEZE subroutine in PLATON.[46] Two benzyl groups are disordered and were held isotropic. All other non-hydrogen atoms were refined anisotropically. No decomposition was observed during data collection. Details of the data collection and refinement are given in the supporting information.

### Crystal data for complex 6

$C_{18}H_{24}N_2Ni_{0.50}P_2$, $M = 359.69$, monoclinic, $a = 9.7763(2)$ Å, $\alpha = 90°$, $b = 19.7795(4)$ Å, $\beta = 101.1210(10)°$, $c = 19.0291(3)$ Å, $\gamma = 90°$, $U = 3610.57(12)$ Å$^3$, $T = 100(2)$ K, space group $C2/c$, $Z = 8$, 10 592 reflections measured, 3181 unique ($R_{int} = 0.0201$) which were used in all calculations. The final w$R(F_2)$ was 0.0804 (all data).

### Crystal data for complex 8

$C_{62}H_{67}B_2F_8N_5NiO_4P_4$, $M = 1302.42$, monoclinic, $a = 24.8972(8)$ Å, $\alpha = 90°$, $b = 11.2331(3)$ Å, $\beta = 113.371(1)°$, $c = 25.3567(8)$ Å, $\gamma = 90°$, $U = 6509.8(3)$ Å$^3$, $T = 90(2)$ K, space group $P2_1/n$, $Z = 4$, 95 676 reflections measured, 11 797 unique ($R_{int} = 0.0409$) which were used in all calculations. The final w$R(F_2)$ was 0.1383 (all data).

## Acknowledgements

This work was supported by the Chemical Sciences program of the Office of Basic Energy Sciences of the Department of Energy. The Pacific Northwest National Laboratory is operated by Battelle for the US Department of Energy. The Bruker (Siemens) SMART APEX diffraction facility was established at the University of Idaho with the assistance of the NSF-EPSCoR program and the M. J. Murdock Charitable Trust, Vancouver, WA, USA.

## References

1 J. C. Fontecilla-Camps, A. Volbeda, C. Cavazza and Y. Nicolet, *Chem. Rev.*, 2007, **107**, 4273–4303; A. Volbeda and J. C. Fontecilla-Camps, *Dalton Trans.*, 2003, 4030–4038; Y. Nicolet, A. L. de Lacey, X. Vernède, V. M. Fernandez, E. C. Hatchikian and J. C. Fontecilla-Camps, *J. Am. Chem. Soc.*, 2001, **123**, 1596–1601; E. Garcin, X. Vernede, E. C. Hatchikian, A. Volbeda, M. Frey and J. C. Fontecilla-Camps, *Structure*, 1999, **7**, 557–565; A. Volbeda, E. Garcin, C. Piras, A. L. de Lacey, V. M. Fernandez, E. C. Hatchikian, M. Frey and J. C. Fontecilla-Camps, *J. Am. Chem. Soc.*, 1996, **118**, 12989–12996.
2 C. Greco, M. Bruschi, L. De Gioia and U. Ryde, *Inorg. Chem.*, 2007, **46**, 5911–5921.
3 H.-J. Fan and M. B. Hall, *J. Am. Chem. Soc.*, 2001, **123**, 3828–3829; A. S. Pandey, T. V. Harris, L. J. Giles, J. W. Peters and R. K. Szilagyi, *J. Am. Chem. Soc.*, 2008, **130**, 4533–4540.
4 A. Silakov, B. Wenk, E. Reijerse and W. Lubitz, *Phys. Chem. Chem. Phys.*, 2009, **11**, 6592–6599.
5 M. Rakowski DuBois and D. L. DuBois, *C. R. Chim.*, 2008, **11**, 805–817; M. Rakowski DuBois and D. L. DuBois, *Chem. Soc. Rev.*, 2009, **38**, 62–72.
6 B. C. H. Steele and A. Heinzel, *Nature*, 2001, **414**, 345–352.
7 J. Zhang, K. Sasaki, E. Sutter and R. R. Adzic, *Science*, 2007, **315**, 220–222.
8 A. Kongkanand, S. Kuwabata, G. Girishkumar and P. Kamat, *Langmuir*, 2006, **22**, 2392–2396.
9 G. Che, B. B. Lakshmi, E. R. Fisher and C. R. Martin, *Nature*, 1998, **393**, 346–349.
10 K. Gong, P. Yu, L. Su, S. Xiong and L. Mao, *J. Phys. Chem. C*, 2007, **111**, 1882–1887.
11 J. Yang, D.-J. Liu, N. N. Kariuki and L. X. Chen, *Chem. Commun.*, 2008, 329–331.
12 B. Winther-Jensen, O. Winther-Jensen, M. Forsyth and D. R. MacFarlane, D. R., *Science*, 2008, **321**, 671–674.
13 K. Gong, F. Du, Z. Xia, M. Durstock and L. Dai, *Science*, 2009, **323**, 760–764.

14 T. Tsukihara, H. Aoyama, E. Yamashita, T. Tomizaki, H. Yamaguchi, K. Shinzawa-Itoh, R. Nakashima, R. Yaono and S. Yoshikawa, *Science*, 1996, **272**, 1136.
15 J. Abramson, M. Svensson-Ek, B. Byrne and S. Iwata, *Biochim. Biophys. Acta, Mol. Cell Res.*, 2001, **1539**, 1.
16 T. Kitagawa and T. Ogura, *Prog. Inorg. Chem.*, 1996, **45**, 431–480.
17 S. Ferguson-Miller and G. T. Babcock, *Chem. Rev.*, 1996, **96**, 2889–2907.
18 J. P. Collman, R. Boulatov, C. J. Sunderland and L. Fu, *Chem. Rev.*, 2004, **104**, 561–588.
19 E. Kim, E. E. Chufán, K. Kamaraj and K. Karlin, *Chem. Rev.*, 2004, **104**, 1077–1133.
20 J. P. Klinman, *Acc. Chem. Res.*, 2007, **40**, 325–333.
21 P. Brzezinski and G. Larsson, *Biochim. Biophys. Acta, Bioenerg.*, 2003, **1605**, 1–13.
22 D. A. Proshlyakov, M. A. Pressler and G. T. Babcock, *Proc. Natl. Acad. Sci. U. S. A.*, 1998, **95**, 8020–8025.
23 A. D. Wilson, R. H. Newell, M. J. McNevin, J. T. Muckerman, M. Rakowski DuBois and D. L. DuBois, *J. Am. Chem. Soc.*, 2006, **128**, 358–366.
24 A. D. Wilson, R. K. Shoemaker, A. Miedaner, J. T. Muckerman, D. L. DuBois and M. Rakowski DuBois, *Proc. Natl. Acad. Sci. U. S. A.*, 2007, **104**, 6951–6956.
25 J. Y. Yang, R. M. Bullock, W. J. Shaw, B. Twamley, K. Fraze, M. Rakowski DuBois and D. L. DuBois, *J. Am. Chem. Soc.*, 2009, **131**, 5935–5945.
26 K. Fraze, A. D. Wilson, A. M. Appel, M. Rakowski DuBois and D. L. DuBois, *Organometallics*, 2007, **26**, 5003–5009.
27 D. E. Berning, A. Miedaner, C. J. Curtis, B. C. Noll, M. Rakowski DuBois and D. L. DuBois, *Organometallics*, 2001, **20**, 1832–1839.
28 V. G. Märkl, G. Y. Jin and C. Schoerner, *Tetrahedron Lett.*, 1980, **21**, 1409–1412.
29 C. J. Curtis, A. Miedaner, R. Ciancanelli, W. W. Ellis, B. C. Noll, M. Rakowski DuBois and D. L. DuBois, *Inorg. Chem.*, 2003, **42**, 216–227.
30 M. T. Kieber-Emmons and C. G. Riordan, *Acc. Chem. Res.*, 2007, **40**, 618–625.
31 I. Kaljurand, A. Kütt, L. Sooväli, T. Rodima, V. Mäemets, I. Leito and I. A. Koppel, *J. Org. Chem.*, 2005, **70**, 1019–1028.
32 Z. M. Heiden and T. B. Rauchfuss, *J. Am. Chem. Soc.*, 2007, **129**, 14303–14310.
33 K. Ishiwata, S. Kuwata and T. Ikariya, *J. Am. Chem. Soc.*, 2009, **131**, 5001–5009.
34 A. D. Wilson, K. Fraze, B. Twamley, S. M. Miller, D. L. DuBois and M. Rakowski DuBois, *J. Am. Chem. Soc.*, 2008, **130**, 1061–1068.
35 J. P. Collman, P. S. Wagenknecht and J. E. Hutchison, *Angew. Chem., Int. Ed. Engl.*, 1994, **33**, 1537–1554; R. Boulatov, J. P. Collman, I. M. Shiryaeva and C. J. Sunderlan, *J. Am. Chem. Soc.*, 2002, **124**, 11923–11935; J. P. Collman, N. K. Devaraj, R. A. Decreau, Y. Yang, Y. Yan, W. Ebina, T. A. Eberspacher and C. E. D. Chidsey, *Science*, 2007, **315**, 1565–1568.
36 Y. Le Mest, C. Inisan, A. Laouenan, M. L'Her, J. Talarmin, M. El Khalifa and J. Y. Saillard, *J. Am. Chem. Soc.*, 1997, **119**, 6095–6106.
37 H.-Y. Lui, I. Abdalmuhdi, C. K. Chang and F. C. Anson, *J. Phys. Chem.*, 1985, **89**, 665–670; C. J. Chang, Y. Deng, D. G. Nocera, C. Shi, F. C. Anson and C. K. Chang, *Chem. Commun.*, 2000, 1355–1356.
38 K. M. Kadish, L. Fremond, J. Shen, P. Chen, K. Ohkubo, S. Fukuzumi, M. El Ojaimi, C. P. Gros, J. M. Barbe and R. Guilard, *Inorg. Chem.*, 2009, **48**, 2571–2582; K. M. Kadish, J. Shen, L. Fremond, P. Chen, M. El Ojaimi, M. Chkounda, C. P. Gros, J. M. Barbe, K. Ohkubo, S. Fukuzumi and R. Guilard, *Inorg. Chem.*, 2008, **47**, 6726–6737; K. M. Kadish, L. Fremond, Z. Ou, J. Shao, C. Shi, F. C. Anson, F. Burdet, C. P. Gros, J. M. Barbe and R. Guilard, *J. Am. Chem. Soc.*, 2005, **127**, 5625–5631; K. M. Kadish, J. Shao, Z. Ou, L. Fremond, R. Zhan, F. Burdet, J.-M. Barbe, C. P. Gros and R. Guilard, *Inorg. Chem.*, 2005, **44**, 6744–6754.
39 C. J. Chang, Z.-H. Loh, C. Shi, F. C. Anson and D. G. Nocera, *J. Am. Chem. Soc.*, 2004, **126**, 10013–10020; J. Rosenthal and D. G. Nocera, *Acc. Chem. Res.*, 2007, **40**, 543–553.
40 J. Y. Yang and D. G. Nocera, D. G., *J. Am. Chem. Soc.*, 2007, **129**, 8192–8198; J. Rosenthal, L. L. Chng, S. D. Fried and D. G. Nocera, *Chem. Commun.*, 2007, 2642–2643; J. D. Soper, S. V. Kryatov, E. V. Rybak-Akimova and D. G. Nocera, *J. Am. Chem. Soc.*, 2007, **129**, 5069–5075; S. Y. Liu and D. G. Nocera, *J. Am. Chem. Soc.*, 2005, **127**, 5278–5279; L. L. Chng, C. J. Chang and D. G. Nocera, *Org. Lett.*, 2003, **5**, 2421–2424.
41 B. J. Hathaway, D. G. Holah and A. E. Underhill, *J. Chem. Soc.*, 1962, 2444–2448.
42 *SMART: v. 5.632*, Bruker AXS, Madison, WI, 2005.
43 *SAINTPlus: v. 7.23a, Data Reduction and Correction Program*, Bruker AXS, Madison, WI, 2004.
44 *SADABS: v.2004/1, an empirical absorption correction program*, Bruker AXS Inc., Madison, WI, 2004.
45 *SHELXTL: v. 6.14, Structure Determination Software Suite*, G. M. Sheldrick, Bruker AXS Inc., Madison, WI, 2004.
46 (*a*) A. L. Spek, *J. Appl. Crystallogr.*, 2003, **36**, 7; (*b*) P. van der Sluis and A. L. Spek, *Acta Crystallogr., Sect. A: Found. Crystallogr.*, 1990, **46**, 194.


 